Tribology International 110 (2017) 35–40

Contents lists available at ScienceDirect

Tribology International

journal homepage: www.elsevier.com/locate/triboint

Operando formation of an ultra-low friction boundary film from synthetic magnesium silicon hydroxide additive

Qiuying Chang[a,*], Pavlo Rudenko[b,c], Dean J. Miller[d], Jianguo Wen[d], Diana Berman[d], Yuepeng Zhang[d], Bruce Arey[e], Zihua Zhu[e], Ali Erdemir[b,*]

[a] School of Mechanical, Electronic and Control Engineering, Beijing Jiaotong University, Beijing 100044, China
[b] Energy Systems Division, Argonne National Laboratory, Argonne, IL 60439, USA
[c] Washington State University, Pullman, WA 99164, USA
[d] Electron Microscopy Center-Center for Nanoscale Materials, Argonne National Laboratory, Argonne, IL 60439, USA
[e] Environmental Molecular Sciences Laboratory, Pacific Northwest National Laboratory, Richland, WA 99354, USA

ARTICLE INFO

Keywords:
Boundary
Thin film
Lubricant additive
Synthetic

ABSTRACT

The paper reports the operando and self-healing formation of DLC films at sliding contact surfaces by the addition of synthetic magnesium silicon hydroxide (MSH) nanoparticles to base oil. The formation of such films leads to a reduction of the coefficient of friction by nearly an order of magnitude and substantially reduces wear losses. The ultralow friction layer characterized by transmission electron microscope (TEM), electron energy loss spectroscopy (EELS), and Raman spectroscopy consists of amorphous DLC containing SiO_x that forms in a continuous and self-repairing manner during operation. This environmentally benign and simple approach offers promise for significant advances in lubrication and reduced energy losses in engines and other mechanical systems.

1. Introduction

A variety of approaches are being explored to reduce friction losses including new low-friction materials [1,2], coatings [3], nanolubrication additives [4–8], ionic liquids [9], charged polymer [10,11] and various low-viscosity base oils. Among these, diamond-like carbon (DLC) coatings have made their way into many industrial applications including hard disk drives, razor blades, engine parts and cutting tools [12]. The term DLC encompasses an array of amorphous carbon coatings and carbon-based nano-structured and nano-composite films [13]. Synthesis of DLC films for industrial applications generally involves plasma-based physical vapor deposition and chemical vapor deposition methods that are expensive and slow (it takes several hours to produce DLC films a few micrometers thick) [14]. Due to their limited thickness, the lifetime of DLC films is finite, and under severe loading situations such films are prone to delamination due to inadequate adhesion or substrate deformation [14]. Clearly it would be highly desirable to produce such DLC films at sliding contact interfaces in a continuous and self-healing manner. In this paper, we describe a novel lubrication approach that leads to in situ and operando formation of such films directly on the contact points where high lubricity and protection against wear are needed. This approach involves the use of a hydrocarbon base oil, such as a pure paraffinic oil, small amounts of MSH nanoparticles and some Ni catalysts.

Base oils used for lubrication provide only moderate protection without additives or some additional protective film on the sliding surfaces. Lubricant additives such as molybdenum dithiocarbamate (MoDTC) and zinc dithiophosphate (ZDDP) have been around for more than 50 years and still are the most important anti-friction and anti-wear additives [15]. MoDTC and ZDDP form slick, highly protective films on rubbing surfaces, but they can poison catalysts and cause environmental pollution [16]. As an alternative to ZDDP or MoDTC additions, addition of carbon nanomaterials such as nano-onions, -tubes or –spheres in colloidal dispersion to carrier oils to form carbon-rich tribofilms on sliding surfaces has been explored. These studies have shown that friction can be substantially reduced and that wear can be highly minimized with the formation of such tribofilms [12]. However, there have been very few attempts to extract similar tribofilms directly from the lubricating oils using catalytically active nanoparticles like those used in this study. Our innovative approach involves the operando formation of carbonaceous coatings by extracting carbon catalytically from the long chain molecules of the hydrocarbon-based carrier oil. This approach is very desirable since it does not rely on the repeated use of expensive, difficult-to-disperse carbon

* Corresponding authors.
E-mail address: qychang@bjtu.edu.cn (Q. Chang).

http://dx.doi.org/10.1016/j.triboint.2017.02.003
Received 15 November 2016; Received in revised form 26 January 2017; Accepted 3 February 2017
Available online 03 February 2017

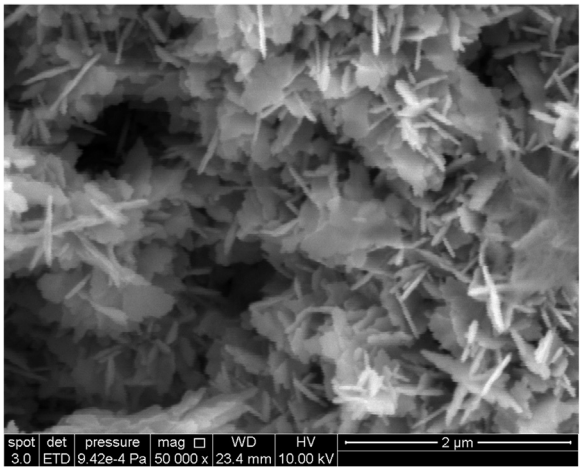

Fig. 1. SEM images of the synthesized MSH powders.

nanomaterials. More importantly, the simple, self-generating and highly adaptive tribolayer is formed directly from the lubricating oil molecules during normal operation of mechanical systems.

2. Experimental and materials

In this work we use synthetically-prepared MSH nanoparticles to achieve compositional uniformity and to add special functionality with the addition of catalytically active dopants (or elements that regulate the catalytic decomposition of oil molecules). The microstructure of the synthetic MSH nanoparticles is characterized by scanning electron microscopy (SEM) in Fig. 1.

For the preparation of the MSH nano-particles, we used a microwave-assisted hydrothermal synthesis process. 10% wt. Ni was doped to the MSH-oil as catalyst. During synthesis, finely ground forsterite and sodium metasilicate particles were mixed in a mechanical mixer and then subjected to a microwave-assisted hydrothermal process at 220 °C for 6 h to form MSH nano-powders. The resulting powders were washed in water for three times to remove sodium and dried in air. Microstructures of MSH were studied using SEM.

The powders were ultrasonically dispersed in polyalphaolefin base oil (PAO) with a viscosity of 32.4 cSt at 40 °C. The resulting oil-MSH suspension/colloid was then used for friction tests. The weight percentage of the powder in the oil-powder suspension was 0.3%. This concentration was optimized in previous studies. At this concentration, the viscosity of the oil was not affected at any measurable level. Friction tests were conducted on a Falex H-60 standard block-on-ring tribometer. The block and ring samples of 52100 steel with 62 HRC hardness were used. The ring rotation speed was 300 rpm and the mechanical load was 300 N, corresponding to a maximum pressure of 0.32 GPa and a speed of 0.549 m/s. Tests were run at room temperature with ~35% RH humidity. A SRV tribometer was used to examine the welding point of the lubricant with MSH. The upper specimen of 52100 steel ball (diameter 12.7 mm) reciprocated on the flat surface of 52100 steel with a frequency of 50 Hz. The stroke length was 5 mm. The load increased from 60 N with a step of 30 N every 2 min. The test stopped automatically as seizure occurred. The same lubricants as above block-on-ring tests were utilized.

TEM specimens were prepared using focused-ion beam approaches. TEM characterization was carried out using the Argonne Chromatic Aberration-corrected TEM (FEI Titan 80-300 ST) with a CEOS spherical and chromatic aberration corrector on the imaging side of the column operated at 80 kV to reduce beam damage to the film.

Chemical analysis of the tribofilm formed during sliding was performed with an Invia confocal Raman microscope using ultraviolet (UV) laser light (λ=325 nm). The UV light was selected in consideration of high sensitivity to carbon species and low fluorescence effect from oil contamination.

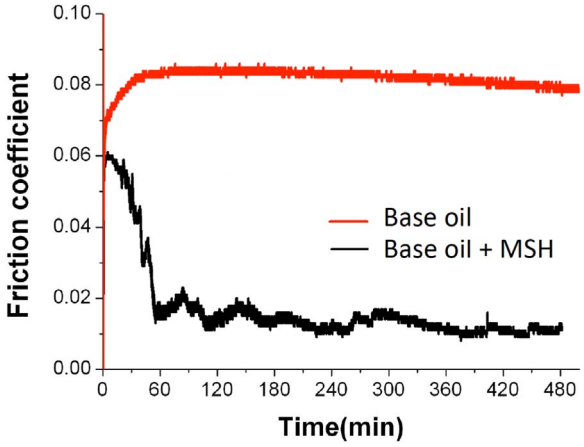

Fig. 2. Evolution of the coefficient of friction (COF) during friction tests for samples lubricated with pure base oil (red line) and the base oil with synthetic magnesium silicon hydroxide (MSH) additives (black line). (For interpretation of the references to color in this figure legend, the reader is referred to the web version of this article).

3. Results and discussion

3.1. Friction and wear

Fig. 2 shows the coefficient of friction (COF) from a steel test pair subjected to friction testing in pure base oil and base oil with the MSH additive (termed as MSH-oil in the following text). The COF of the sample tested in pure base oil is ~0.08 at steady state and remains steady until the end of the test. In contrast, the COF of the sample tested in MSH-oil decreases dramatically from an initial level of ~0.06 to ~0.01 at steady state. The dramatic decrease of friction during the initial run-in period is most likely due to the formation of a carbon-rich tribolayer on the rubbing surfaces. We believe a tribolayer forms first locally at asperity tips and then gradually expands in size and eventually covers the entire contact surface. After the tribolayer becomes continuous (after about 60 min), the COF begins to stabilize but still fluctuates occasionally between 0.02 and 0.01. Such fluctuations in COF with time are likely due to a self-generation and -organization mechanism of a low-shear tribolayer. The presence of a carbon-rich protective tribolayer on the samples tested with MSH additive was confirmed by electron microscopy, and Raman spectroscopy.

Fig. 3 shows plan-view optical microscopy images and 3D depth profiles of the wear grooves formed on the block side of the samples. The sample that was lubricated with MSH-oil had much narrower and smoother wear surface as compared to the sample that was tested in base oil. In addition, the wear groove for the MSH-oil lubricated sample was half depth of that for the sample tested in pure base oil, as shown in the 3D depth profiles. A grayish tribofilm on the rubbing surfaces of both block and ring samples was apparent. These results show that the addition of synthetic MSH leads to remarkably superior antiwear performance.

We used the thermoelastohydrodynamic lubrication (TEHL) model given in [17] to estimate the oil film between the block and ring under the same conditions as the above block/ring test, and the film thickness over contact area is between 0.14 μm and 0.08 μm shown in Fig. 4. The X axis and Y axis correspond to ring axial direction and ring rotating direction respectively in Fig. 4. The roughness of the wear track in the presence of MSH is about 0.1 μm. So the ratio of film thickness and roughness is between 1.4 and 0.8 which indicates the mixed lubrication occurs. Hence, we should not attribute the low friction to the pure hydrodynamic lubrication. From another aspect, the fluctuation of COF

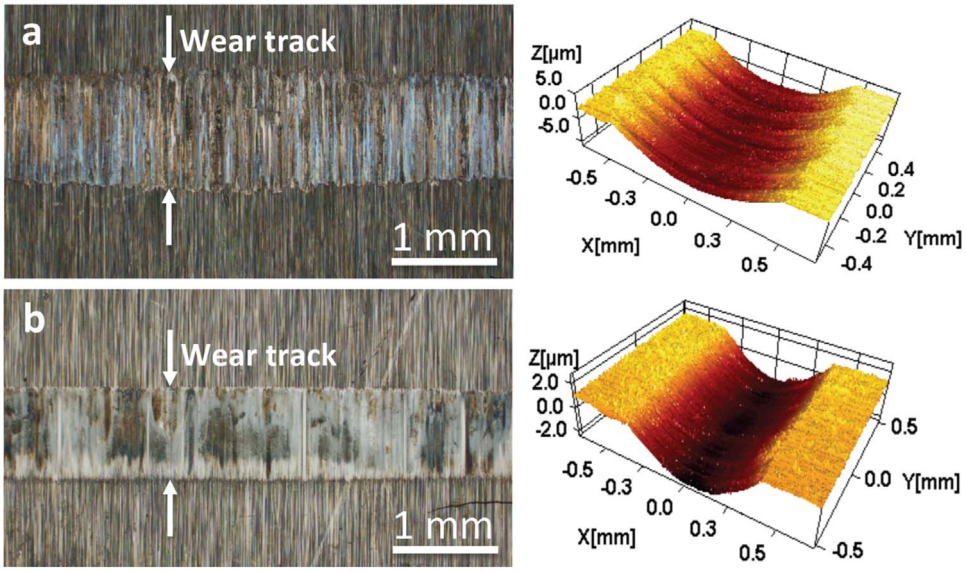

Fig. 3. Optical images and depth profiles of the friction surface of the specimens Images are from a sample lubricated with (a) pure base oil and (b) base oil with MSH additive. Depth profile of the friction surface of the specimens tested using (c) pure base oil and (d) base oil with MSH additive.

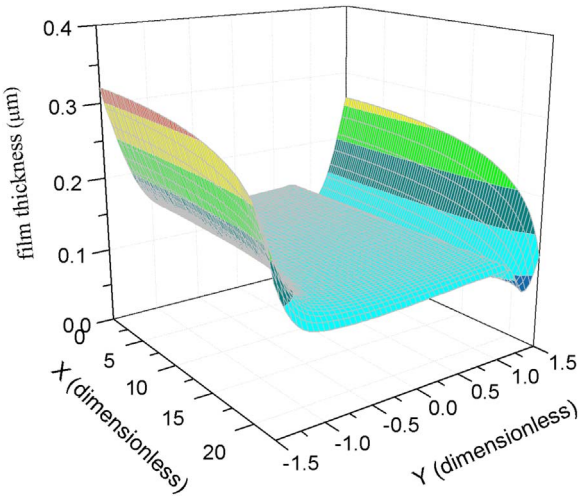

Fig. 4. Film thickness of block and ring tribopair simulated with TEHL model under the same conditions as block/ring test.

curve further indicates the boundary films contact directly, otherwise, the COF would keep steady in hydrodynamic lubricating regime.

The red line in Fig. 5 presents the load steps. The black curve shows

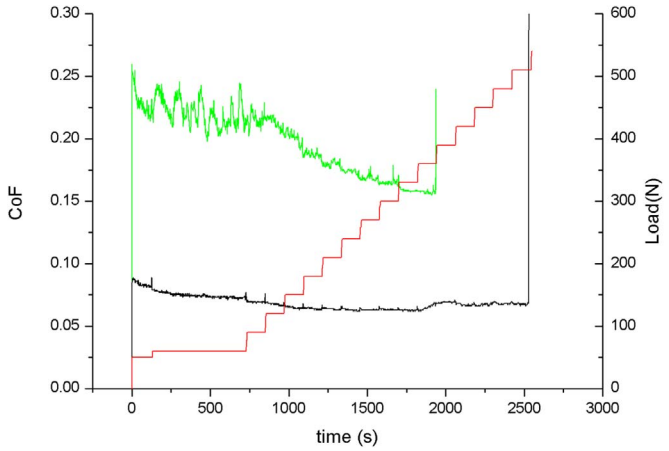

Fig. 5. Welding points of MSH-oil and PAO base oil measured with a SRV tribometer.

us COF of the tribopair lubricated with MSH-oil. The contact surface scuffed when the load increased to 500 N. Before scuffing the COF keeps a low and steady value , even at the beginning of the test. In Contrast, the COF in base oil without MSH represented by green curve waves dramatically in the beginning of the test which implies a severe wear occurring and decreases from 0.25 to 0.15 with the contact area increasing resulted from wear. And the tribopair lubricated with base oil welded around 300 N which is much lower than that in MSH-oil. From the high extreme pressure value of MSH-oil we can further conclude that a film with low friction and excellent anti-wear properties formed.

3.2. Surface analysis

The TEM image in Fig. 6a confirms the existence of a continuous tribolayer with a thickness of 15–30 nm. And the tribofilm has a layered structure. This is further confirmed by high-angle annular dark-field (HAADF) imaging, as shown in Fig. 6b. The HAADF image was collected with a large cut-off collection angle (~100 mrad) so the intensity of the image is mainly Z-contrast. The dark layers in Fig. 6b consist of light elements. Phases composed of high Z elements, such as the steel substrate and the Pt coating, are bright in the image. A closer look at the tribofilm using High-resolution TEM (HRTEM) in Fig. 6c reveals that the dark layers shown in Fig. 6a are nanocrystalline while the brighter layers are featureless, suggesting an amorphous like structure. Energy Dispersive X-ray Spectroscopy (EDS) analysis of the entire tribofilm shown in Fig. 7 reveals that it consists primarily of carbon and oxygen, but also contains magnesium, silicon, and iron. The synthetic MSH additive is a source for magnesium and silicon. HRTEM images and electron diffraction show no evidence of residual synthetic MSH phases within the tribofilm, indicating that the synthetic MSH decomposed under the combination of mechanical and thermal energy during the tribological test. It has been shown that MSH dehydrates (or dehydroxylates) easily – even at low shear force – and hydroxyl groups are released [18–21]. This also leads to shear weakening of the dehydrated MSH phase and amorphization. Thus, decomposition of the MSH is not surprising.

The nature of the topmost layer of a tribofilm is critical to the tribological performance, and we found that the topmost layer of the tribofilms in this study was always amorphous. Electron energy-loss spectra (EELS) in the low-loss (Fig. 6d) and high-loss (Fig. 6e) regimes show that the composition of the amorphous phase is mainly carbon,

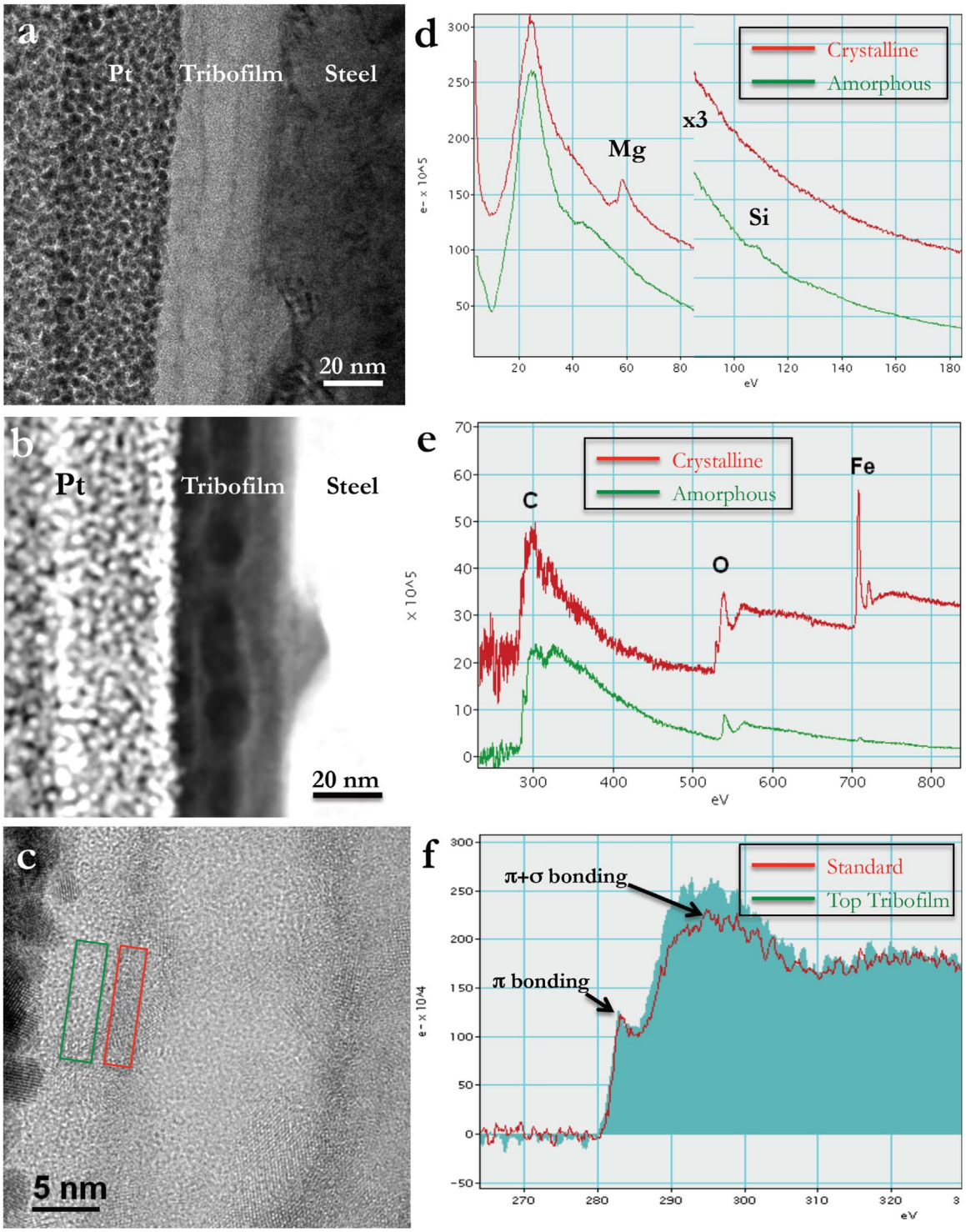

Fig. 6. TEM images at the topmost of tribofilm. (a) Cross-sectional TEM image and (b) HAADF image of a tribofilm formed during friction tests with the addition of MSH nanoparticles. (c) HRTEM image of tribofilm showing amorphous and crystalline layers. EELS spectra for amorphous and crystalline areas at (d) low- and (e) high-loss regimes, (f) Comparison between carbon K-edge EELS spectra of the topmost amorphous tribofilm and the standard amorphous carbon film with 100% sp^2 ratio. The Pt protective layer was deposited to protect the tribolayer from damage during TEM specimen preparation.

oxygen, and silicon while that of the crystalline phase is primarily iron, oxygen, and magnesium. The oxygen K-edge from the crystalline areas shows very different features than the amorphous regions (Fig. 6e) – the three oxygen peaks probed from a crystalline area are characteristic of iron oxides [22]; the two peaks and a sudden rise of the oxygen K-edge at the amorphous area correspond to silica [23]. This data suggests that the topmost wear layer consists of amorphous carbon and some SiO_x. The bonding of the amorphous carbon is analyzed by comparing the sp^2 ratio of its carbon K-edge to a standard amorphous carbon film with 100% sp^2 ratio. sp^2 ratio in the top amorphous carbon layer of the tribofilm is calculated using the pre-edge peak intensity of a carbon K edge (around an energy loss of 283 eV) since the pre-edge peak is contributed only from sp^2-bonded electrons (π bonding). All carbon atoms are sp^3 bonded in diamond and all sp^2 bonded in graphite. So, diamond shows no pre-edge peak and graphite shows maximum pre-edge peak. To avoid strong dependence of pre-edge peak

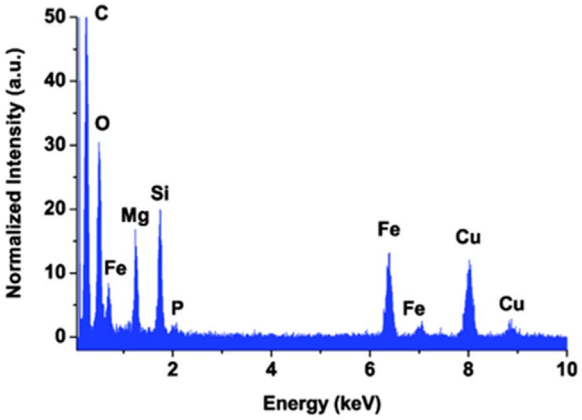

Fig. 7. EDS spectra from the tribofilm.

intensity on crystalline orientation, an amorphous carbon film sputtered in argon at room temperature is used as a standard instead of crystalline highly ordered pyrolytic graphite. Fig. 6f shows two EELS spectra from the standard sample and the top amorphous layer of the tribofilm. Two EELS spectra were collected at the same conditions, using low lose of 80 kV electrons to avoid knock-out damage to graphite film. The electron dose is kept below 1×10^6 e/Å^2. To avoid beam damage as pointed out by Liao et al. [23]. Both spectra were background subtracted and deconvoluted to remove multiple scattering using their corresponding zero-loss peaks. The sp^2 ratio is calculated to be ~80% using the Gaussian peak fitting, suggesting a DLC-like nature of the layer [24].

Confocal Raman spectroscopy provides additional insight into the nature of the tribofilm. Fig. 8 shows Raman spectra from the wear track debris (Fig. 8a) and a region outside of the wear track area (Fig. 8b) for comparison. The spectrum from the wear track exhibits the characteristic D and G peaks (at ~1374 and ~1602 cm^{-1}, respectively) that are typical for DLC films [25]. Raman mapping that shows the intensity distribution of the D and G peaks and indicates that the wear track is rich in carbon (Fig. 8d and e). The intensity ratio I_D/I_G, which was relatively constant at ~0.5 over the wear track area, confirms the formation of diamond-like carbon that is a mixture of sp^2-bonded amorphous carbon (a-C) (presence of G peak) and sp^3-bonded tetrahedral amorphous carbon (ta-C) (presence of D peak). More accurate quantitative carbon sp^3 contribution was estimated from the T peak (~1085 cm^{-1}, present due to sp^3 sites) [26] in UV Raman spectra. The intensity ratio I_T/I_D of ~10% indicates low sp^3 content in the DLC films of ~20%, which is consistent with the EELS analysis. Based on these results, we conclude that the impressive friction and wear performance (see Figs. 2 and 3) is due to formation of a DLC film with unique tribological properties during operation.

We believe that the in-situ formation of the tribofilm relies on the extraction of carbon from the lubricant by nickel dopants in the synthetic MSH and that the incorporation of SiO_x into the DLC-like tribolayer provides enhanced wear properties. It has been shown that the combination of silicon or hydroxyl groups with carbon stabilizes DLC and decreases friction significantly [27]. The addition of SiO_x to a-C or ta-C has the beneficial effects of reducing the grown-in compressive stress, improving thermal stability, and maintaining low COF to a higher relative humidity [28–30]. Since Si only bonds to sp^3, its incorporation causes shrinkage of the C sp^2 clusters and opens the C sp^2 rings [31]. The complex layered structure of the tribofilm suggests the interplay of several different processes in its formation and growth. Our data suggests that following the initial attachment of an MSH particle to the steel/iron oxide surface, a pressure-induced decomposition process occurs. SiO_x released by this decomposition can react with amorphous carbon extracted from the base oil, leading to the formation of a complex DLC layer with ultra-low friction.

4. Conclusion

In conclusion, we have demonstrated operando formation of a dual-phase tribofilm using synthetically manufactured nanoparticles as an oil additive, resulting in a striking reduction in sliding friction. The ultralow friction is attributed to the formation of a surface layer in the tribofilm that consists of amorphous DLC that also contains SiO_x. This surface layer forms in a continuous and self-repairing manner during operation. Synthetic MSH provides a favorable structure for the introduction of metallic carbonization catalysts and Mg, OH, and Si that are important to the formation of the DLC layer. Furthermore, this approach is economical and easily deployed in commercial systems. Future work aims to optimize such a lubrication system, which could lead to significant advances in the lubrication field and have a significant, positive impact on energy efficiency and the durability of engines and other mechanical components.

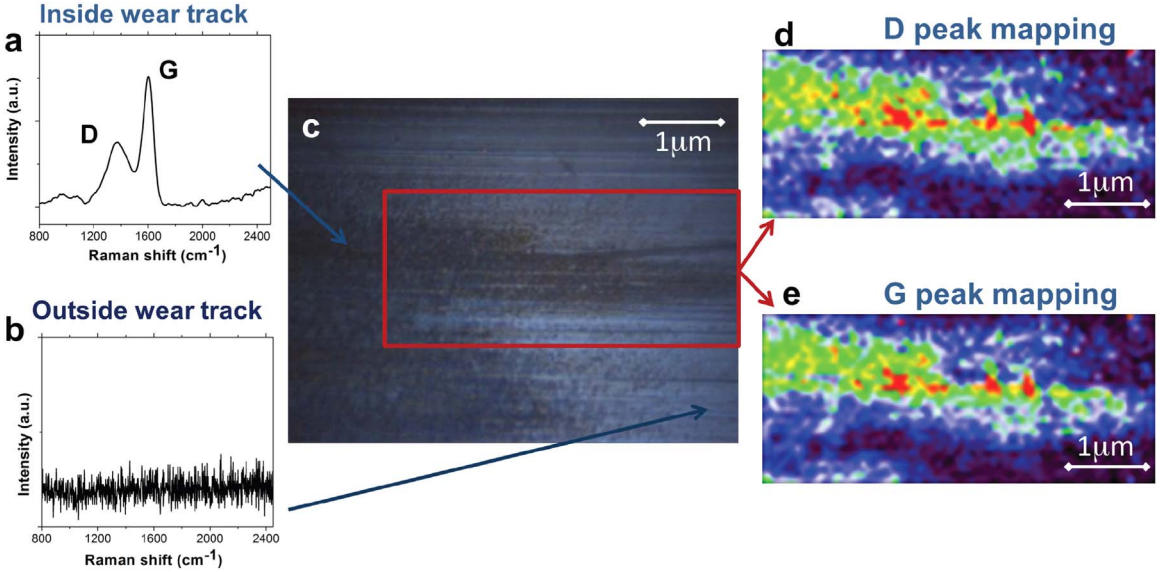

Fig. 8. Raman spectra of topmost tribofilm (a) Raman spectrum of topmost tribofilm formed in lubricant with synthetic MSH additives (b) Raman mapping using D-band at 1374 cm^{-1} over area of about 20 μm ×10 μm. (c) Raman mapping using G-band at 1604 cm^{-1} over the same area as (b). (Red color corresponds to the highest intensity, blue to the lowest when no peak is present). (For interpretation of the references to color in this figure legend, the reader is referred to the web version of this article).

Acknowledgements

Qiuying Chang thanks the National Science Foundation of China (NSFC) on grant number 51075026 and the Tribology Science Fund of State Key Laboratory of Tribology (SKLTKF12B02). Research carried out in the Electron Microscopy Center – Center for Nanoscale Materials was supported by the U.S. Department of Energy, Office of Science, Office of Basic Energy Sciences, under Contract no. DEAC02-06CH11357. Pavlo Rudenko is also thankful for partial support from the Hydropower Research Foundation funded by DOE, NASA Space Grant and SBIR Phase I Award number 1315855 from US National Science Foundation.

References

[1] Nosonovsky M. Materials science: slippery when wetted. Nature 2011;477:412–3. http://dx.doi.org/10.1038/477412a.
[2] Matsumoto N, Mistry KK, Kim J-H, Eryilmaz OL, Erdemir A, Kinoshita H, et al. Friction reducing properties of onion-like carbon based lubricant under high contact pressure. Tribol – Mater Surf Interfaces 2012;6:116–20. http://dx.doi.org/10.1179/1751584×12Y.0000000014.
[3] Bhushan B, Gupta BK. Handbook of tribology: materials, coatings, and surface treatments. New York, NY (United States): McGraw-Hill; 1991.
[4] Martin JM, Ohmae N. Nanolubricants. West Sussex, England: John Wiley & Sons; 2008.
[5] Rapoport L, Bilik Y, Feldman Y, Homyonfer M, Cohen SR, Tenne R. Hollow nanoparticles of WS2 as potential solid-state lubricants. Nature 1997;387:791–3. http://dx.doi.org/10.1088/0957-4484/18/11/115703.
[6] Chhowalla M, Amaratunga G. Thin films of fullerene-like MoS2 nanoparticles with ultra-low friction and wear. Nature 2000;407:164–7. http://dx.doi.org/10.1038/35025020.
[7] Rudenko P, Bandyopadhyay A. Talc as friction reducing additive to lubricating oil. Appl Surf Sci 2013;276:383–9. http://dx.doi.org/10.1016/j.apsusc.2013.03.102.
[8] Bhushan B, Israelachvili JN, Landman U. Nanotribology: friction, wear and lubrication at the atomic scale. Nature 1995;374:607–16. http://dx.doi.org/10.1038/374607a0.
[9] Minami I. Ionic liquids in tribology. Molecules 2009;14:2286–305. http://dx.doi.org/10.3390/molecules14062286.
[10] Raviv U, Giasson S, Kampf N, Gohy J-F, Jérôme R, Klein J. Lubrication by charged polymers. Nature 2003;425:163–5. http://dx.doi.org/10.1038/nature01970.
[11] Chen M, Briscoe WH, Armes SP, Klein J. Lubrication at physiological pressures by polyzwitterionic brushes. Science 2009;323:1698–701. http://dx.doi.org/10.1126/science.1169399.
[12] Erdemir A, Donnet C. Tribology of diamond-like carbon films: recent progress and future prospects. J Phys D Appl Phys 2006;39:R311–R327. http://dx.doi.org/10.1088/0022-3727/39/18/R01.
[13] Robertson J. Diamond-like amorphous carbon. Mater Sci Eng R Rep 2002;37:129–281. http://dx.doi.org/10.1016/S0927-796X(02)00005-0.
[14] Donnet C, Erdemir A. Tribology of diamond-like carbon films: fundamentals and applications; 2007. Springer; New York, NY, United States.
[15] Rudnick LR. Lubricant additives: chemistry and applications, second edition. Boca Raton, FL, United States: CRC Press; 2009.
[16] Rokosz MJ, Chen AE, Lowe-Ma CK, Kucherov AV, Benson D, Paputa Peck MC, et al. Characterization of phosphorus-poisoned automotive exhaust catalysts. Appl Catal B Environ 2001;33:205–15. http://dx.doi.org/10.1016/S0926-3373(01)00165-5.
[17] Liu X, Yang P. Analysis of the thermal elastohydrodynamic lubrication of a finite line contact. Tribol. Int. 2002;35:137–44.
[18] Viti C, Hirose T. Dehydration reactions and micro/nanostructures in experimentally-deformed serpentinites. Contrib Miner Pet 2009;157:327–38. http://dx.doi.org/10.1007/s00410-008-0337-6.
[19] Lin A, Takano S, Hirono T, Kanagawa K. Coseismic dehydration of serpentinite: evidence from high-velocity friction experiments. Chem Geol 2013;344:50–62. http://dx.doi.org/10.1016/j.chemgeo.2013.02.013.
[20] Weber JN, Greer RT. Dehydration of serpentine: heat of reaction and reaction kinetics at PH2O=1atm. Am Miner 1963,;50:450–64.
[21] Hirose T, Bystricky M, Kunze K, Stünitz H. Semi-brittle flow during dehydration of lizardite-chrysotile serpentinite deformed in torsion: implications for the rheology of oceanic lithosphere. Earth Planet Sci Lett 2006;249:484–93. http://dx.doi.org/10.1016/j.epsl.2006.07.014.
[22] Seto Y, Sakamoto N, Fujino K, Kaito T, Oikawa T, Yurimoto H. Mineralogical characterization of a unique material having heavy oxygen isotope anomaly in matrix of the primitive carbonaceous chondrite Acfer 094. Geochim Cosmochim Acta 2008;72:2723–34. http://dx.doi.org/10.1016/j.gca.2008.03.010.
[23] Muller DA, Sorsch T, Moccio S, Baumann FH, Evans-Lutterodt K, Timp G. The electronic structure at the atomic scale of ultrathin gate oxides. Nature 1999;399:758–61. http://dx.doi.org/10.1038/21602.
[24] Liao Y, Pourzal R, Wimmer MA, Jacobs JJ, Fischer A, Marks LD. Graphitic tribological layers in metal-on-metal hip replacements. Science (80-) 2011;334:1687–90. http://dx.doi.org/10.1126/science.1213902.
[25] Ferrari A, Robertson J. Interpretation of Raman spectra of disordered and amorphous carbon. Phys Rev B 2000;61:14095–107. http://dx.doi.org/10.1103/PhysRevB.61.14095.
[26] Ferrari AC, Robertson J. Raman spectroscopy of amorphous, nanostructured, diamond-like carbon, and nanodiamond. Philos Trans A Math Phys Eng Sci 2004;362:2477–512. http://dx.doi.org/10.1098/rsta.2004.1452.
[27] Kano M, Yasuda Y, Okamoto Y, Mabuchi Y, Hamada T, Ueno T, et al. Ultralow friction of DLC in presence of glycerol mono-oleate (GMO). Tribol Lett 2005;18:245–51. http://dx.doi.org/10.1007/s11249-004-2749-4.
[28] Ikeyama M, Nakao S, Miyagawa Y, Miyagawa S. Effects of Si content in DLC films on their friction and wear properties. Surf Coat Technol 2005;191:38–42. http://dx.doi.org/10.1016/j.surfcoat.2004.08.075.
[29] Santra TS, Liu CH, Bhattacharyya TK, Patel P, Barik TK. Characterization of diamond-like nanocomposite thin films grown by plasma enhanced chemical vapor deposition. J Appl Phys 2010;107:124320. http://dx.doi.org/10.1063/1.3415548.
[30] Bhaskaran H, Gotsmann B, Sebastian A, Drechsler U, Lantz MA, Despont M, et al. Ultralow nanoscale wear through atom-by-atom attrition in silicon-containing diamond-like carbon. Nat Nanotechnol 2010;5:181–5. http://dx.doi.org/10.1038/nnano.2010.3.
[31] Prawer S, Nemanich RJ. Raman spectroscopy of diamond and doped diamond. Philos Trans A Math Phys Eng Sci 2004;362:2537–65. http://dx.doi.org/10.1098/rsta.2004.1451.